Three characterisations of 3D reconstruction uncertainty with bounded error

Benoît Telle*, Olivier Stasse†, Toshio Ueshiba*, Kazuhito Yokoi†, Fumiaki Tomita*
AIST/IS 3D Vision Group , AIST/IS-CNRS/STIC Joint Japanese-French Robotics Laboratory (JRL)†*
Intelligent Systems Research Institute (IS),
National Institute of Advanced Industrial Science and Technology (AIST)
AIST Central 2, Umezono 1-1-1, Tsukuba, Ibaraki, 305-8568 Japan
{benoit.telle,olivier.stasse,kazuhito.yokoi,t.ueshiba,f.tomita}@aist.go.jp

***Abstract*— Considering a stereoscopic visual system, this paper deals with the error involved by a 3D reconstruction process. If image pixels are seen as surfaces instead of points, interval analysis provides bounding boxes in which the reconstructed 3D point lies with certainity. This paper presents a method which refine this bounding box and gives a tighter approximation of the error. Using bissection, and a reprojection test in the image planes, the space in which the 3D reconstructed point may be located is given as an octree. This is achieved through the resolution of a set inversion problem using the SIVIA algorithm. For a lighter manipulation of the result, an englobing ellipsoid is deduced from this approximation. Finally the three models are tested on a recognition process for a humanoid robot.**

***Index Terms*— 3D reconstruction, bissection, ellipsoids**

I. Introduction

This paper deals with the uncertainty related to the 3D reconstruction problem. There are three sources of error in general : the segmentation process, the chosen parameters in the camera model, and the pixel information. Taking into account this error may be done through an additive term to the pixels position, the camera model or both. The Gaussian distribution has been extensivly used as such additive term, and the applications include calibration process [1] [2], motion estimation [3], environment modeling [4], self localization applied to robots [5], registration [6], or visual servoing [7]. A statistical study on the influence of modelization by Gaussian noise can be found in [8], but is also possible to solve the 3D reconstruction problem using Interval Analysis as proposed in [9] and [10]. The latter approach provided a upper bounded evaluation of the error and does not need a sufficient number of samples to be statistically representative. An application using this approach to build partial boundaries representation of objects is proposed in [11]. However the main inconvenient of this method is the limitation related to the geometrical shape of the intervals. Indeed the results provided may be seen as a bounding box of the true shape of the reconstruction error. This problem is known as the wrapping effect [12]. In this regard, the method proposed provides the optimal bounding box of this space. But if such a space is very close to the diagonal of its bounding box, then a better geometrical representation has to be find. Unfortunatly the work on uncertainty using Gaussian distribution clearly show that this is the case for the 3D reconstruction problem. Following the work of Jaulin [13], this paper describes a method to obtain a tighter approximation of this error using a paving representation. In our application, the paving is the union of intervals which follow a particular subdivision scheme and representend by a 8-tree called octree. The core idea of this reconstruction is to solve a set inversion problem using the property of the uncertain based model projection. Finally as octrees are not handy to represent large numbers of error spaces, for instance in the context of disparity maps, it is proposed to build bounding ellipsoids. The remainder of this paper is organized as follows: Section II introduces the camera model used in the framework of Interval Analysis. Section III recalls briefly how the reconstruction problem is solved using intervals. Section IV explains how the paving representation is build. Section V details how a bounded ellipsoid is build on the resulting octree. Finally section VI provides some results in the context of a research behavior.

II. Camera Model

The most popular camera model in computer vision is the pinhole model. It allows to use the projective geometry properties; thus the projection observed by a camera is a linear application given by Eq. (1). This model has 12 degrees of freedom. The complete projection of a scene point Q_h through the camera model is given by [14][15]:

$$q = PQ_h = K\,(R|t)\,Q_h \tag{1}$$

where K is the matrix of intrinsic parameters, $(R|t)$ is the matrix of extrinsic parameters. R represents the orientation of the camera in the scene frame, and t is its position. Q_h is a 4 dimensional homogeneous vector of a 3 dimensional point in the scene. Matrix P represents the linear application associated to the projection, its dimension is (3×4), and q is the homogeneous vector associated to the image point of Q_h by P. In the following, we consider the error relative to the projection of a 3D point in the image plane. Classically this error add a Gaussian term to the projection defined by Eq. 1. In this paper, we deal with bounded error by using the alternative model proposed in [11] which represents each pixel by an interval. Computation with intervals is a common way to make guarranted calculus in numerical computation, and the detailed rules of this

arithmetic is given in [13]. Vision problems reformulated in the framework of interval analysis is presented extensively in [9]. Thus only pertinent concepts and tools related to this field will be introduced.

The uncertainty associated to the position of an image point is introduced as the interval vector $[\varepsilon]$. The projection is now written:

$$[q] = E\left(\frac{PQ_h}{P_3^t Q_h}\right) + [\varepsilon] \tag{2}$$

Where E is the round operator which furnishes the nearest integer of a value. The denominator $P_3^t Q_h$ is the normalisation of data description in the image, where P_3 is the third column of the camera model P. This allows to fix the scale factor and to define the error vector: $[\varepsilon] = \begin{pmatrix} [\varepsilon_1] & [\varepsilon_2] & 0 \end{pmatrix}^t$. According to the model, there is no error on the scale factor, but only an uncertainty on the position of the geometric point in the image plane. $[q]$ is the resulting interval vector. Values of $[q]$ describes the boundaries of the projections of the 3D point in the image plane.

A. 3D reconstruction

Concerning a stereoscopic system, a couple of camera, represented by P_l,P_r, compensates the not full rank relation in the algebraic representation given by Eq. 1. Indeed, the relation between a 3D point and its couple of projections provides the following over-determined system:

$$\begin{pmatrix} q_l \\ q_r \end{pmatrix} = \begin{pmatrix} P_l \\ P_r \end{pmatrix} Q_h \tag{3}$$

We observe 6 equations and 4 unknown data. It represents the intersection of the two reprojected lines defined by the center of each camera and each image point. The resolution of this linear system furnishes the coordinate of the 3D reconstructed point. It is equivalent to an over-determined system in the form:

$$AQ_{nh} = B \tag{4}$$

Matrix A and vector B are build with the elements of P_l, P_r, q_l and q_r. Q_{nh} is the non homogeneous vector of the 3D point in the scene. Due to the projective representation of space, it is given up to a scale factor [10][14][15].

B. Handling data uncertainty

Using equation 2, the pixels position are described with intervals $([q_l],[q_r])$. From [10] it provides the system (equation 4) based on interval arithmetics rules. First, the matrix P associated to a camera model is cut such as:

$$P = (M \mid V) \tag{5}$$

Where M is a (3×3) matrix and V is a (3×1) vector. From Eq. 5, and by introducing the operator $[*]_\times$ then the system to solve (Eq. 4) may be written in the interval analysis framework as:

$$[A]\,Q_{nh} = [B] \tag{6}$$

with

$$[A] = \begin{pmatrix} [[q_l]]_\times M_l \\ [[q_r]]_\times M_r \end{pmatrix}; [B] = \begin{pmatrix} [[q_l]]_\times V_l \\ [[q_r]]_\times V_r \end{pmatrix} \tag{7}$$

where $[A]$ is an interval matrix, $[B]$ an interval vector, and $[*]_\times$ the cross product function. This operator gives the associate anti-symmetrical matrix. For a given interval vector this operator is such as: $([a][b][c])^t$

$$\left[\begin{pmatrix}[a]\\[b]\\[c]\end{pmatrix}\right]_\times \mapsto \begin{pmatrix} 0 & [-c] & [b] \\ [c] & 0 & [-a] \\ [-b] & [a] & 0 \end{pmatrix}$$

The exact set of 3D points $\{Q_s\}$ which is solution of the uncertain linear system is :

$$\{Q_s\} = \left\{Q_{nh} \in \mathbb{R}^3 | \exists A \in [A], \exists B \in [B], AQ_{nh} = B\right\} \tag{8}$$

In the next section we briefly introduce tools of interval analysis providing a minimal external bounding box $[X] = [\{Q_s\}]$ of $\{Q_s\}$. This is the first characterisation of the bounded error related to the 3D reconstruction in this paper.

III. Bounding box for 3D reconstruction error

In the framework of interval analysis, linear system such as Eq. 8 can be solved using a *fixed point contractor* [13]. The use of this tool has been developed in computer vision in [11]. Applied to the linear system given by Eq. 8 it provides a box $[Q_s]$ which contains the solution set $\{Q_s\}$ such as:

$$[Q_s] \quad = [\{Q_{nh} | \exists A \in [A], \exists B \in [B], AQ_{nh} = B\}] \tag{9}$$

Let's call $\mathcal{C}_{GS}$ the Gauss-Siedel fixed point contractor and $\mathcal{C}_K$ the Krawczyk fixed point contractor. Both seek for the minimal $[X_s]$ such as:

$$\begin{array}{ll} \{Q_s\} & \subset [Q_s] = \mathcal{C}_{GS}([A],[B]) \\ \{Q_s\} & \subset [Q_s] = \mathcal{C}_K([A],[B]) \end{array} \tag{10}$$

Applying these operators solve the linear system 7 for a couple of calibrated camera and a set of matched points. In [11] a comparison is given which led us to chose the Gauss Siedel contractor as it provides a good trade-off between accuracy and speed. The results applied to a real scene depicted in Fig. 1 are represented in Fig. 2. Data are provided by the VVV system [16]. This versatile system using a trinocular stereo camera setup is able to reconstruct 3D information of a scene, to recognise an object [17], to track a recognised object [18], and to build a model using a range finder system. The boxes represent the intervals in which lie the features points. The uncertainty which have been taken into account is digitalisation noise: $[\varepsilon] = ([-0.5,0.5][-0.5,0.5][0^-,0^+])^t$. As expected, due to the geometric model of the camera, deeper objects, or objects far away from the optical axis intersection are less precisely located.

IV. Paving of 3D reconstruction error

The previous approach provides a bounding box of the set $\{Q_S\}$. However considering Eq. 8, and the fact that we are using a bounding box, several points does not fullfill the property stated by Eq. 4. This problem is known as the wrapping effect [12]. Indeed the geometry of the box does not map the true shape of $\{Q_s\}$. Then in this

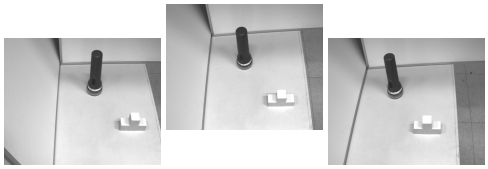

Fig. 1. Original images for 3D reconstruction. 2 kinds of objects are considered: Geometrical form and free form.

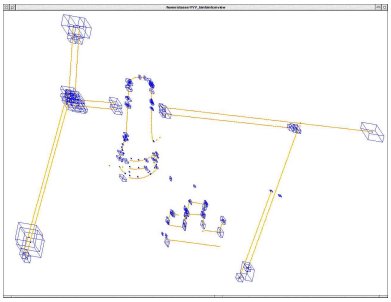

Fig. 2. Viewpoint of a 3D reconstruction with Boundaries representation and interval bounding boxes. Only digitalisation noise is taken into account.

section a new geometrical approximation based on paving is proposed. It builds a better approximation which still bound the real solution $\{Q_s\}$.

We propose here to consider the projection in a set inversion problem. Indeed, we can say that reconstruction consists in searching the set of 3D points $\{Q_s\}$ such as their projection obtained with the n cameras P_i $(i = 1...n)$ are the pixels image $[q_i]$ $(i = 1...n)$. By using the model of camera we proposed (Eq. 2), we can write the following relation:

$$Q_h \in \{Q_s\} \quad \Rightarrow \quad \left\{ E\left(\frac{P_i Q_h}{P_{i3}^t Q_h}\right) + [\varepsilon] \right\} \in [q_i] \quad \text{for } i = 1...n \tag{11}$$

Let us now introduce the problem of set inversion. It consists in retrieving the domain of definition of a given function when the image domain is known.

A. Definitions for Set inversion

Let f be a function from $\mathbb{R}^m$ to $\mathbb{R}^n$ and $\mathbb{Y}$ a subset of $\mathbb{R}^n$. Set inversion is the characterisation of $\mathbb{X}$ such as:

$$\mathbb{X} = \{x \in \mathbb{R}^m | f(x) \in \mathbb{Y}\} = f^{-1}(\mathbb{Y}) \tag{12}$$

Lets call $[f]$ the inclusion function of f defined with the following properties:

$$\forall [x] \in \mathbb{IR}^m,\ f([x]) \subset [f]([x]) \tag{13}$$

If

$$[f]([x]) = f([x]) \tag{14}$$

then $[f]$ is the optimal inclusion function associated to f.

Under the condition that the inclusion function $[f]$ of f is convergent, the algorithm SIVIA, developed by Jaulin [13] allows us to find $\mathbb{X}$ with interval analysis. Convergence is defined as following:

Definition 1: Let $[x]_k$ be a series of intervals defined on $\mathbb{X}$, the inclusion function $[f]$ defined on $\mathbb{X}$ is *convergent* if and only if:

$$\lim_{k\to\infty} (rad([x]_k)) \to 0 \Rightarrow \lim_{k\to\infty} (rad([f]([x]_k))) \to 0 \tag{15}$$

B. Application to 3D reconstruction

In our case, the inclusion function $[f]$ is based on the projection model without error entries, the round operator $E()$ and the additive uncertainty introduces in Eq. 2. Then given a set of cameras P_i, $\mathbb{X}$ is the 3D uncertain point we are looking for $\mathbb{X} = \{Q_s\}$:

$$f_i(Q_h) = \frac{P_i Q_h}{P_{i3}^t Q_h} \tag{16}$$

$$[f_i]([Q_h]) = \frac{P_i [Q_h]}{P_{i3}^t [Q_h]} \tag{17}$$

The numerator is a linear application, so $P_i[Q_h]$ is an optimal inclusion function and is convergent [10]. So does the denominator $P_{i3}^t[Q_h]$. The property of convergence of $[f_i]$ is conditioned by the value of this ratio. With a calibrated cameras, we use to obtain $s \in P_{i3}^t[Q_h]$ and $s \neq 0$. Then let choose a series $[Q_h]_k$ of intervals such as :

$$\lim_{k\to\infty} (rad([Q_h]_k)) \to 0 \tag{18}$$

$$\forall k,\ s \in [Q_h]_k \ and\ s \neq 0 \tag{19}$$

We can bound the value of each dimension of $[f_i]([Q_h])$ with two series which converge to a same point. Then it demonstrates that $[f]([Q_h])$ is convergent. Indeed:

$$\frac{inf(P_i[Q_h]_k)}{s + 2rad(P_{i3}^t[Q_h]_k)} \leq [f_i]([Q_h]_k) \leq \frac{sup(P_i[Q_h]_k)}{s - 2rad(P_{i3}^t[Q_h]_k)} \tag{20}$$

Set inversion algorithm with interval analysis is based on the subdivision of a set of intervals which estimate the set $\{Q_s\}$. In our application, this upper bounded estimation is provided as the result of the contractor.

C. Paving and sub-paving

The paving is a collection of subsets without overlapping such as their union is an approximation of the space $\{Q_s\}$. Let us call $\widehat{\{Q_s\}}_0$ the initial approximation of the space $\{Q_s\}$ defined by:

$$\widehat{\{Q_s\}}_0 = [Q_s] \tag{21}$$

The image space $\mathbb{Y}$ is the known set of pixels $[q_i]$ (Eq.11) which are the images of $\{Q_s\}$ throught the differents cameras P_i.

$$\mathbb{Y} = \{\cup_i [q_i]\} \tag{22}$$

The SIVIA algorithm is used to construct iteratively the paving of the approximation of space $\{Q_s\}$ using an inclusion test and a partionning of the space $\widehat{\{Q_s\}}_0$. Considering the SIVIA algorithm at iteration k the approximation of

$\{Q_s\}$ is the union of intervals $[Q_h]_j$ elements of $\widehat{\{Q_s\}}_0$ defined by:

$$\widehat{\{Q_s\}}_k = \{\cup_j [Q_h]_j \mid [f_i]([Q_h]_j) \cap [q_i] \neq \{\emptyset\}\} \quad (23)$$

The inclusion test consists in verifying if the image of $[Q_h]_j$ through the inclusion functions of the projection $[f_i]$ intersect the pixel $[q_i]$. Then three cases are possible: the intersection is empty, the intersection is complete, and the intersection is partial (neither empty nor complete). In the first case, the interval is discarded. In the second case, the interval is included in the approximation of $\{Q_s\}$. In the third case, the interval needs further refinement. To perform this refinement, the interval is splitted in eight intervals, and the SIVIA algorithm is performed recursively on those intervals. The splitting operation is called **BISSECTION**. The subdivision in eight three-dimensional intervals corresponds to a well-known data structure in computer graphics called the octree.

Algorithm 1 is our adaptation of SIVIA algorythm to 3D reconstruction problem. The variable ε is the precision of the reconstruction we want. This variable allows us to control the depth of the octree. Indeed given the fact that any interval $[Q_h]$ is splitted by two in the three directions while using BISSECTION, and that the initial bounding box is $[Q_s]$, then the maximal depth of the octree and ε are related as follows:

$$\frac{min_{d=\{1,2,3\}} rad_d([Q_s])}{2^{depth-1}} < \varepsilon \quad (24)$$

With $rad_d([Q_s])$ the radius of the interval $[Q_s]$ along the dimension d. The algorythm is first call with $[Q_h] = [Q_s]$ and $\widehat{\{Q_s\}} = \{\emptyset\}$.

Algorithm 1 SIVIA $\left(\text{in} : [f_i], [Q_h], [q_i], \varepsilon;\ \text{in-out} : \widehat{\{Q_s\}}\right)$

if $(\exists i \mid [f_i]([Q_h]) \cap [q_i] = \{\emptyset\})$ **then**
  Return
else
  if $(\forall i\ ,\ [f_i]([Q_h]) \subset [q_i])$ **then**
    $\widehat{\{Q_s\}} := \widehat{\{Q_s\}} \cup [Q_h]$
    Return
  else
    if $\left(\frac{min_{d=\{1,2,3\}} rad_d([Q_s])}{2^{depth-1}} < \varepsilon\right)$ **then**
      $\widehat{\{Q_s\}} := \widehat{\{Q_s\}} \cup [Q_h]$
      Return
    else
      $[Q_h]_{j=1...8} = BISSECTION([Q_h])$
      for $j = 1:8$ **do**
        $\widehat{\{Q_s\}} := \widehat{\{Q_s\}} \cup \text{SIVIA}\left([f_i], [Q_h]_j, [q_i], \varepsilon, \widehat{\{Q_s\}}\right)$
      end for
    end if
  end if
end if

Also an octree is adaptated to the implementation of this algorithm, its is difficult to use in the context of a vision based robotic application. For instance, considering a disparity map, it would be a burden to have an octree for each reconstructed point. Thus in the next section, from this representation, an ellipsoid including an octree associated to each 3D point is computed in order to provide a light representation of the uncertainty related to the 3D reconstructed point.

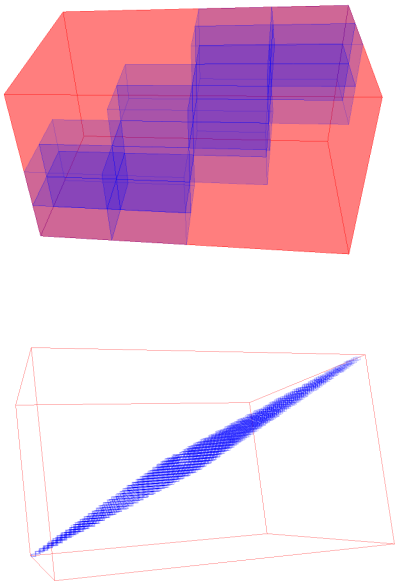

Fig. 3. bissection

V. Bounding ellipsoid representation

Octrees are a very convenient structure for describing 3D space. Nevertheless the manipulation of a set of octrees for geometric computations is not so comfortable. Here is shown a method which permit to compute the bounding ellipsoid for a set of point. This method will be applied to the octree we obtained in the previous stage. The "bounding ellipsoid" (or "minimal spanning ellipsoid") is the smallest volume ellipsoid that contains a set of point $\{Q_s\}$. It can have any orientation. Thus, it also is a very tight approximation for the object it contains, and is an excellent container. Also, it is not difficult to test inclusion of a point in an ellipsoid.

A. Data to be used from the octree representation

The next step is to use the information provided by the bissection to compute the ellipsoid. The goal is to extract points from the previously computed octree. Two kinds of points are available for each subspace containing some information: the centres and the extremities (figure 5). The main problem related to the center is the possibility to lose some information because the surrounding volume of those centres has been ignored. Thus using the subspace extremities make sure that the overall subspace will be included in the computed ellipsoid. Indeed as the ellipsoid and the subspace are convexes if the ellipsoid include the extremities of the subspace it includes also the subspace.The possible drawback related to the use of

subspace extremities is their redundancy. Indeed if they belong to adjacent rectangles containing information, they are counted once for each of such rectangle. Hopefully, this can be regarded as a weighted average. This process gives more weight to the area included inside the space, and less to its borders.

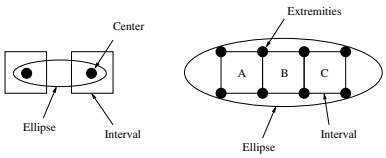

Fig. 4. Ellipse construction - In the left part of the figure points are taken into account only once but ellipse does not fit the whole intervals. In the right part of the figure, points which belongs to intervals A and B or B and C are taken into account twice.

B. Computation of a bouding ellipsoid

For a set of non-collinear points (non-planar in 3D) the bounding ellipsoid exists and is unique. [19] gives a fast randomised algorithm for computing the bounding ellipsoid. Fast implementation has been developed [20]. In the case of 3 dimensional ellipsoid, the method proposed here is a suboptimal solution. It is derived from statistical theory and/or mechanical ones. It is known that the representation of the covariance matrix for a set of point is an ellipsoid. The tensor of inertia for a set of points with equal mass has the same expression (up to a scale factor). Then let us write $\{Q\}$ a set of n points choosen in the set $\{Q_s\}$, Q_i one of its point and $\overline{Q}$ the gravity center or the mean of $\{Q\}$. Tensor of inertia and covariance matrix of this set is based on the following matrix:

$$E_0 = \sum_i \left(Q_i - \overline{Q}\right)^t \left(Q_i - \overline{Q}\right) \tag{25}$$

E_0 is a quadratic form. Covariance matrix scales E_0 by the square inverse of the number of element in $\{Q\}$ (ie n^{-2}), inertia matrix by the mass of the element. We aims to compute the smallest bounding ellipsoid E which contain the whole set of point. We scale E_0 in order to fit E. The scale factor is defined by the point Q_{far} the most far from the center of the distribution.

$$E = \frac{1}{\left(Q_{far} - \overline{Q}\right)^t E_0 \left(Q_{far} - \overline{Q}\right)} E_0 \tag{26}$$

Indeed, this scale factor ensure inclusion of the cloud $\{Q\}$ in the ellipsoid E. We can verify:

$$\forall Q_i \in \{Q\} \ , \ \left(Q_i - \overline{Q}\right)^t E \left(Q_i - \overline{Q}\right) \leq 1 \tag{27}$$

Let be $\{Q\}$ be the set of points Q_i given by the cloud of extremal points for a given octree. It has been seen that covariance matrix is given by :

$$E_0 = \sum_i \frac{(Q_i - \overline{Q})(Q_i - \overline{Q})^T}{n^2} \tag{28}$$

Where $n = Card(\{Q\})$, and $\overline{Q}$ is the average. It has been shown that this scale is not necessary, it allows us to use weights for redundant points. To enclose all the points inside one ellipse, this initial matrix is scaled as it is shown in Eq. 26. Scale factor is defined as S such as:

$$S = \max_i \left(Q_i^T E_0 Q_i\right) \tag{29}$$

Then the ellipsoid is expanded in the following manner:

$$E = \frac{1}{S} E_0. \tag{30}$$

The result of the previously described computation for an octree is depicted in Fig. 5. It is possible to remark first that the bounding box is not so pessimistic compare to the real intersection volume. But the interval cannot be oriented in order to fit better the real uncertain area. It illustrates wrapping effect problem [12]. In comparison, modifying depth of the octree allows to have a relatively accurate description of the 3D reconstruction using the proposed algorithm. At last, the ellipsoid is a trustworthy representation of the uncertainty domain.

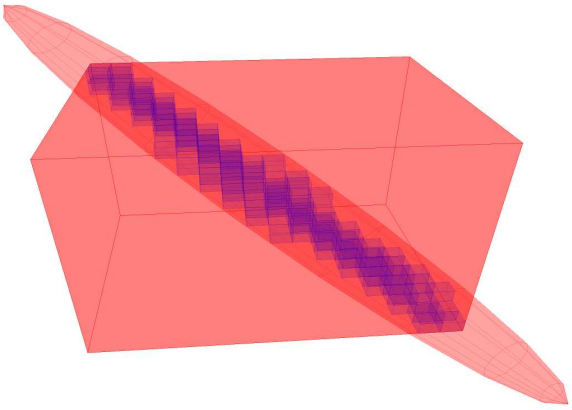

Fig. 5. Results of the SIVIA algorithm on the reconstructed point. The true shape of the error space has been approximated by an octree. The bounding box illustrate the result of the fixed point contractor. The surrounding ellipsoid build on the octree is also depicted.

VI. Experiment

This method has been applied in the context of a recognition process described in [21] applied to the humanoid robot HRP-2 [22]. This process is based on the comparison between 3D lines detected in the environment and a CAD-like 3D model. The previously described method has been used to compute the error of reconstructed 3D points. The object looked for is a T-shaped depicted in Fig. 6. The 3

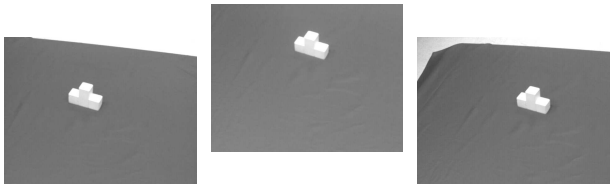

Fig. 6. Original images for 3D reconstruction. In this context the T-Shape is the object to recognise.

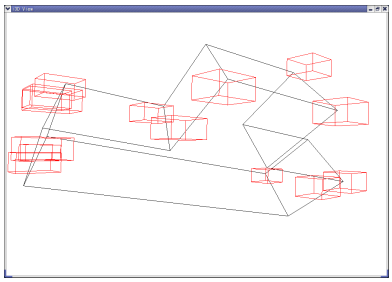

(a) Bounding box of the error

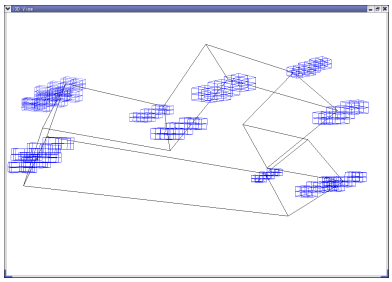

(b) Paving of the error space

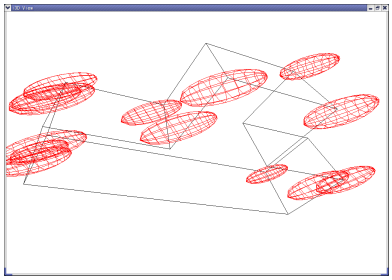

(c) Bounding ellipsoid for the error space

Fig. 7. The three models detailed in the text are represented: the bounding box, the paving, and the bounding ellipsoid. Different viewpoints of some 3D points reconstructed and used in the recognition process. For sake of visibility, the selected 3D points are the extremities of the edges detected. Only digitalisation noise is taken into account.

different boundaries are displayed in Fig. 7. The depth of the octree is 2, and the computation takes 1.3 seconds on 24 points using a Pentium IV 1.7 Ghz. The T shape displayed in Fig. 7 is the model with the position and the orientation computed by [21]. Also such computation seems to not fit a real-time process, using a resolution similar to the one used in compression (127×74 for instance) and a look-up-table implementation of the results computed off-line, it might be possible to have a description of the error related to the stereoscopic system to be used at frame-rate.
For sake of visibility, the 3D points displayed in Fig.7 are only the extremities of none adjacent segments. We can remark that not all the edges are detected. Indeed not all the object parts are visible from the viewpoint displayed in Fig. 6. Moreover, some real edges are not fully detected which explain why some points are on the edges but not at the extremities on the model.

VII. Conclusion

This paper has proposed a new method to build an upper bounded approximation of the 3D reconstruction error. Using a recursive constructive approach with the SIVIA algorithm, it is possible to have a better geometric model of the error space. As this approximation use a data structure which may not be efficient for dealing with large set of data, a bounding ellipsoid may be constructed. This bounding ellipsoid is still an upper bound of the reconstruction error. This work may be used to compare bounded error approach with results obtained while considering a probabilistic framework. Finally this approach has been illustrated in the context of a recognition process.

References

[1] Z. Zhang, "A flexible new technique for camera calibration," *IEEE Transaction on Pattern Analysis and Machine Intelligence*, vol. 22(11), no. MSR-TR-98-71, pp. 1330–1334, 2000.

[2] Zhang, "Determining the epipolar geometry and its uncertainty: A review," *International Journal of Computer Vision*, vol. 27(2), pp. 161–198, 1998.

[3] C. Zeller and O. Faugeras, "Camera self-calibration from video sequences: The kruppa equations revisited," INRIA, Tech. Rep. RR2793, 1996.

[4] F.-X. Espiau and P. Rives, "Extracting robust features and 3d reconstruction in water images," in *OCEAN*. Hawaii: MTS/IEEE, 2001.

[5] G. Borges and M. Aldon, "Robust estimation algorithm for mobile robot localization on geometrical environment maps," *To appear in Robotics and Autonomous Systems*, 2004.

[6] L. Douadi, "Recalage de nuage de points 3d fournis par un capteur embarqué," LIRMM, Tech. Rep., 2002.

[7] P. Rives, "Visual servoing based on epipolar geometry," in *International Conference on Intelligent Robots and Systems (IROS), Takamatsu, Japan*, 2000.

[8] E. Grossmann and J. S. Victor, "The precision of 3d reconstruction from uncalibrated views," in *British Machine Vision Conference*, 1998.

[9] B. Telle, M. J. Aldon, and N. Ramdani, "Guaranted 3d visual sensing based on interval analysis," in *Proceedings IROS*, 2003.

[10] B. Telle, "Méthode ensembliste pour une reconstruction 3d garantie par stereo vision," Ph.D. dissertation, Université Montpellier II, 2003.

[11] B. Telle, O. Stasse, T. Ueshiba, K. Yokoi, and F. Tomita, "3d boundaries partial representation of objects using interval analysis," in *inproceedings IROS 2004*, november 2004.

[12] R. Moore, *Interval Analysis*. Englewood Cliffs: Prentice-Hall, 1966.

[13] L. Jaulin, M. Kieffer, O. Didrit, and E. Walter, *Applied Interval Analysis*. London: Springer Verlag, 2001.

[14] O. Faugeras, *Three Dimensional Computer Vision*. MIT press, 1992.

[15] R. Hartley and A. Zisserman, *Multiple View Geometry in Computer Vision*. Cambridge, 2001.

[16] K. Kaneko, F. Kanehiro, S. Kajita, K. Yokoyama, K. Akachi, T. Kawasaki, S. Ota, and T. Isozumi, "Design of prototype humanoid robotics platform for hrp," October 2002.

[17] Y. Sumi, Y. Kawai, T. Yoshimi, and F. Tomita, "Recognition of 3d free-form objects using segment-based stereo vision," in *International Conference on Computer Vision*, 1998.

[18] Y. Sumi, Y. Y. Ishiyama, and F. Tomita, "Hyper frame vision: A real-time vision system for 6-dof object localization," in *International Conference on Pattern Recognition*, 2002.

[19] E. Welzl, "Smallest enclosing disks (balls and ellipsoids)," *New Results and New Trends in Computer Science, Lecture Notes in Computer Science*, vol. 555, pp. 359–370, 1991.

[20] B. Gartner and S. Schonherr, "Smallest enclosing ellipses - fast and exact," Free Univ. Berlin, Tech. Rep., 1997.

[21] Y. Sumi, Y. Kawai, T.Yoshimi, and T. Tomita, "3d object recognition in cluttered environments by segment-based stereo vision," *International Journal of Computer Vision*, vol. 6, January 2002.

[22] K.Kaneko, F.Kanehiro, S.Kajita, H.Hirukawa, T.Kawasaki, M.Hirata, K.Akachi, and T.Isozumi, "Humanoid robot hrp-2," in *Proceedings of the 2004 IEEE International Conference on Robotics & Automation*, 2004.